



45th SME North American Manufacturing Research Conference, NAMRC 45, LA, USA

Coated tool Performance in Dry Turning of Super Duplex Stainless Steel

Rajaguru J^{a*} and Arunachalam N^b

^a Research scholar, Department of mechanical engineering, IIT madras, Chennai, Tamil Nadu, 600036, India

^b Assistant professor, Department of mechanical engineering, IIT madras, Chennai, Tamil Nadu, 600036, India

Abstract

Super duplex stainless steels (SDSS) are widely used in marine environments because of their excellent mechanical properties and corrosion resistance. The presence of different alloying elements and their two phase microstructure makes it a difficult-to-machine material. The use of multilayer coated cutting tools is an effective strategy to improve the cutting performance during dry machining of this material. In this work, the performance of four different coated tools made either by PVD or CVD has been investigated during dry turning of SDSS. Their performances were evaluated in terms of tool wear, cutting force, cutting temperature and surface integrity. Results indicated that [MT-TiCN]-Al₂O₃ coating provided relatively better performance than other coatings in terms of tool wear, cutting force and surface integrity. Their combined properties of higher hardness and oxidation stability make them an effective coating during machining. The TiN-[MT-TiCN]-Al₂O₃ coating exhibited higher tool wear, poor surface finish and also less tensile residual stress in comparison with surfaces machined using other coated tools. This may be due to the dominance of plastic deformation by mechanical load over temperature effects during machining.

© 2017 Published by Elsevier B.V. This is an open access article under the CC BY-NC-ND license (<http://creativecommons.org/licenses/by-nc-nd/4.0/>).

Peer-review under responsibility of the organizing committee of the 45th SME North American Manufacturing Research Conference

Keywords: SDSS; Medium Temperature-CVD; Multilayer coatings; Surface Integrity

1. Introduction

Duplex stainless steels are called "duplex" because they have a two phase microstructure with 50 % ferrite and 50% austenite. It is designed for demanding applications which requires exceptional mechanical strength and corrosion resistance such as, heat exchangers, desalination plant, seawater equipment, oil and gas exploration component. The SDSS is characterized by its higher chromium content (25%) than the standard duplex stainless steel (20%) with pitting resistant equivalent > 40 (PREN = Cr% + 3.3Mo% + 16N %). Increasing their alloying elements chromium, molybdenum, and nitrogen increases the resistance to localized corrosion and stress corrosion cracking. The poor machinability of this material is due to very low heat conductivity (50% of that of plain carbon steels), high toughness, high tendency to form built up edge (BUE) and high work hardening rate [1-2]. The

presence of two phases austenite and ferrite with different hardness also makes them difficult-to-machine. The high heat generated at the tool chip interface combined with the low thermal conductivity of this material produces high localized temperatures which causes rapid tool wear. Nomani et al. (2013) compared the machinability behavior of super duplex SAF 2507, duplex SAF 2205 and austenite 316L in drilling process. The results showed that austenite 316 had better machinability and both duplex grades have a higher response to built-up edge formation, with grade 2507 being the worst. These poor machinability features of this material define the need to improve the machinability of this material.

Multilayer coatings and delivering coolant in the cutting zone are the two effective ways to enhance the cutting performance. The coating layer enhances the surface properties of tools such as wear resistance, hot hardness, oxidation resistance and chemical inertness, which augments the tool life [4]. The common techniques used for coating of cutting inserts include physical vapor deposition and chemical vapor deposition. More recently, medium temperature CVD (MT-CVD) process has also been developed, where the deposition of thin films are done at temperature between 700 °C and 850°C. These coatings have lower tensile thermal stress and have reduced tendency to form brittle η -phase at the interface of substrate and thin film [5-6]. These advancement in coatings technology helps to machine the complicated materials at high cutting speeds and feeds, which could help to increase the productivity. Krolczyk et.al (2014) investigated tool wear of CVD coated tungsten carbides in duplex stainless steel (DSS) turning. In this work two different multilayer coatings TiCN/Al₂O₃/TiN and TiN/ Ti(C,N)/ Ti(N,B)/ TiN/ Ti(C,N) were used, the former showed higher resistance to abrasive wear. Peng et.al (2014) studied the effect of single layer TiAlN and multilayer TiN/TiAlN coatings on the oxidation performance. It was found that TiN layer insertion into the TiAlN coating hinders the Al diffusion and enhances the oxidation resistance at the surface. Chen et.al (2011) prepared TiAlN/TiN nano-multilayer coatings with modulation period of ~20 nm in order to further improve the properties of TiN coating. The multilayer structure resulted in an increase in adhesion with substrate and improved oxidation resistance, which improved the overall cutting performance of insert. Ciftci et.al (2006) performed dry turning experiments on AISI 304 and AISI 316 austenitic stainless steels and the results showed TiC/TiCN/TiN coated cutting tools produced lower cutting forces than TiCN/TiC/Al₂O₃ coated tools, because of the lower coefficient of friction of TiN top coating layer. Bejjnai et al (2016) did the characterization on worn surfaces of alumina coatings of insert for different work piece materials. White light interferometry was used to study the grooves found on the flank side after machining. Park et al (2011) performed flank wear analysis on the multi-layer (TiCN/Al₂O₃/TiCN) coated carbide inserts after turning AISI 1045 steel. Using the wavelet filtering, the roughness profiles and groove sizes on the flank surface were also analyzed and compared with confocal laser scanning microscope (CLSM) and SEM. This review indicates the machining problems in SDSS and the need to develop a suitable strategy to improve the machinability. Hence, this present work includes analyzing the comparative performance of different coated tools in SDSS turning. Their performances were assessed in terms of tool wear, cutting force, cutting temperature and surface integrity.

2. Materials and Methods

The material used in this study SDSS has an approximately equal proportion of 50% ferrite and 50 % austenite and its microstructure is shown in Fig 1. The ultimate tensile strength was found to be UTS = 910 MPA with a Rockwell hardness of 32 HRC. The elemental composition of SDSS of grade 2507 is shown in Table 1.

Table 1. Chemical composition of SDSS

Element	C	N	Si	P	S	Cr	Mn	Ni	Mo	Fe
Wt%	0.03	0.25	2.06	0.03	0.02	24.6	1.20	6.1	4.00	Remaining

The turning experiments were performed on a VDF lathe under dry conditions. It offers a variable speed from 150- 5600 rpm with the power rating of 10 kW. Tungsten carbide cutting insert with geometry of TNMG 160408 MP clamped in the tool shank of MTJNR2525M16H4 were used and the details of insert coating is given below in Table 2. The ranges of cutting conditions were chosen based on the industrial recommendations. The process

parameters were kept constant throughout this study with the cutting velocity= 120 m/min, feed=0.3 mm/rev and depth of cut =1 mm.

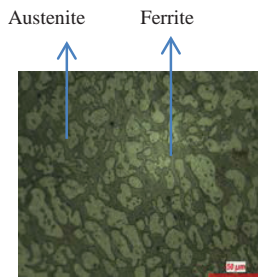
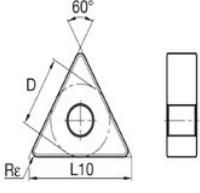


Fig. 1. SDSS Microstructure

Table 2. Insert specification and multilayer coated tool details

Insert details	Tool	Coatings	Coating technique
Geometry-TNMG 160408 MP  D -9.53 mm L -16.50 mm Re-0.8 mm	1	AlTiN - (2 μm)	PVD
	2	MT-TiCN (top) - (2 μm) Al ₂ O ₃ (bottom) - (1.5 μm)	CVD
	3	TiN (top) - (2 μm) MT-TiCN - (2 μm) Al ₂ O ₃ (bottom) - (1.5 μm)	CVD
	4	TiOCN (top) - (2 μm) Al ₂ O ₃ - (1.5 μm) TiCN - (1.5 μm) MT-TiCN - (2 μm) TiN (bottom) - (2 μm)	PVD

With this constant set of process parameters and same tool geometry, performance of the different coatings were evaluated in terms of cutting forces, cutting temperature, the tool wear and the surface integrity. The measurements of cutting force along the 'x' and 'z' axes (F_x , &, F_z) are carried out with Kistler piezoelectric 9257B three component dynamometer and charge amplifier of type 5015A. The data acquisition was accomplished using Labview software. The sampling rate of 150 Hz was used to collect data. Infrared-camera, FLIR T250, with a maximum temperature range of 1200° C was used to measure dynamic cutting temperature at the tool work piece interface. Samples were examined under the SEM and 3D non-contact profilometer to study the wear mechanisms of inserts and work piece surface roughness after machining. To analyze the elemental distribution of the coated tools Energy Dispersive Spectroscopy (EDS) analysis has been carried out after machining. The mapping of elements by this technique helps in better understanding of coating layer behavior. The machining induced residual stresses on the surface is measured by X-ray diffraction (XRD) technique at ferrite peak (211) with an X-ray radiation source of Cr-Kβ. The flank wear studies on different coatings were done with a span of different machining length 15 cm, 30 cm, 45 cm and 60 cm. The cutting force, cutting temperature were collected during initial machining length of 15 cm. EDS analysis on worn out edges, surface roughness and residual stress measurements were also made on the work surface after machining initial 15 cm length for tool and the work piece.

3. Results and Discussion

3.1 Tool Wear

The flank wear of different coating tool were analyzed after machining with fresh tool tip. The AlTiN coated tool provided better initial wear resistance up to 45 cm of machining length as shown Fig.2. This may be due to the formation of Al₂O₃ layer when the coating is exposed to high temperature as shown in Fig. 5 (a). The dense Al₂O₃ layer retards the diffusion of oxygen into the surface and provides superior oxidation resistance. Their extreme hardness at high temperature and low thermal conductivity also provided much needed stability in dry machining. Fig 3. (a) shows the wear in the flank face caused by abrasion and adhesion. It also indicates high amount of built-up edge formation along the edge that could also have protected cutting edges against wear. However, once that single layer gets completely worn out, the tungsten carbide particles are exposed after 60 cm machining length as shown in Fig. 4 (a). The EDS analysis confirms the depletion of AlTiN layer, as the elemental distribution in Fig. 4 (b) shows

tungsten along the cutting edges. Soon after that flank wear rate increased and reached a higher value. The detachment of particles due to higher built-up edge also resulted in increased flank wear.

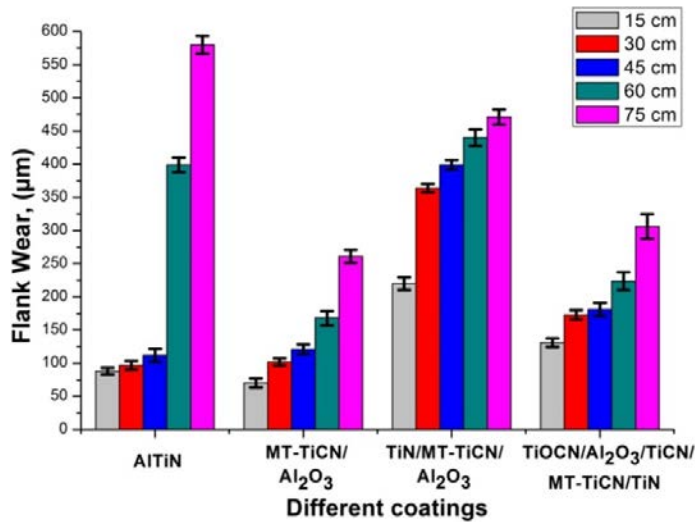


Fig. 2. Flank wear behaviour of different coatings

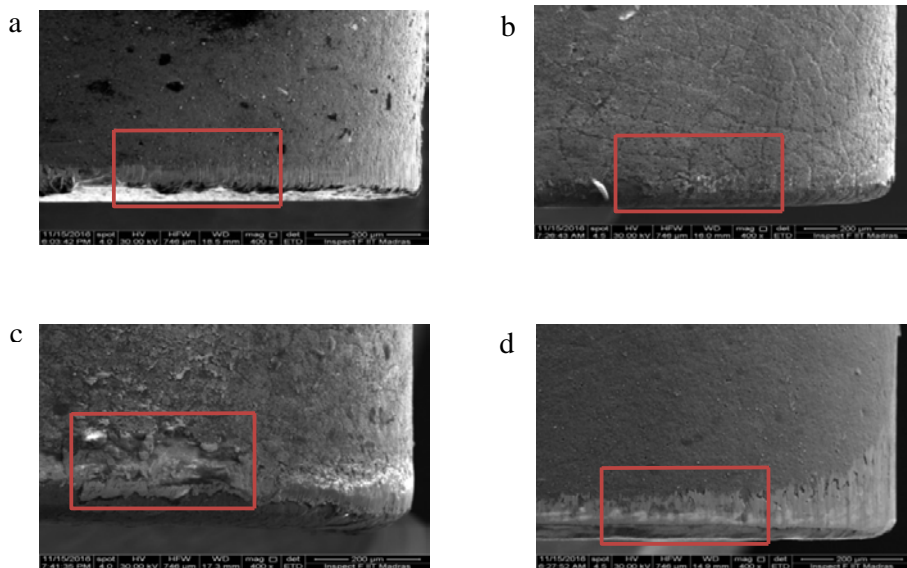


Fig. 3. SEM images of different coatings after 15 cm machining length

[MT-TiCN]-Al₂O₃ provided better wear resistance throughout the machining process than the three other coatings. The combined effect of high hardness by MT-TiCN and oxidation resistance by Al₂O₃ at the interface resulted in better wear resistance as shown in Fig. 3 (b). This coating behaved better among all coatings in terms of flank wear. Fig. 6 (a) depicts the formation of aluminum oxide along the cutting edge. It indicates the counteracting effects of Al₂O₃ layer in providing oxidation resistance. Fig. 6 (c) shows the no tungsten being exposed along the

cutting edges. The top layer TiCN made by medium temperature CVD with less internal stress in the layer aids in reduction of cracking caused by thermal loads that further provides better thermal stability.

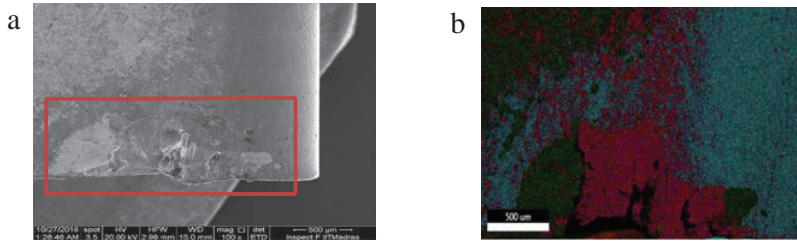


Fig. 4. SEM image (a) & EDS analysis (b) of AlTiN coating after 60 cm machining length
W- ■ , Fe- ■ element

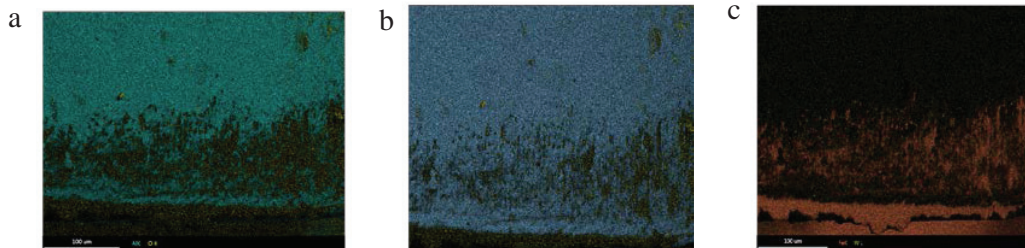


Fig. 5. EDS showing the elemental mapping for the ROI (red box) coating AlTiN :
(a)Al- ■ , O- ■ (b) Ti- ■ , O- ■ (c) Fe- ■ , W- ■

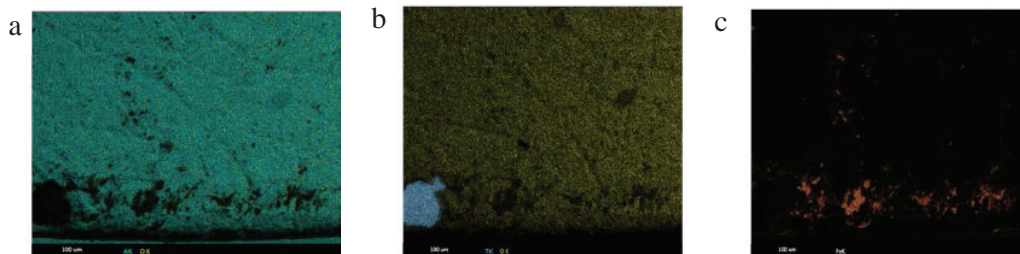


Fig. 6. EDS showing the elemental mapping for ROI (red box) the coating [MT-TiCN]- Al₂O₃:
(a)Al- ■ , O- ■ (b) Ti- ■ , O- ■ (c) Fe- ■ , W- ■

The TiN-[MT-TiCN]-Al₂O₃ coating exhibited non-uniform wear and performed poorly among all the four different coatings. The top Ti-N coating has lower hardness and this layer along with the second layer [MT-TiCN] could have enhanced the titanium to diffuse towards the top surface over the aluminum. This resulted in titanium oxide layer formation at the top that allows the oxygen to penetrate into the TiN layer and generate pores in their layer. Thicker the oxide layer, higher the compressive stresses developed which also lead to reduced adhesion of TiN layer and cracking of Al₂O₃ layer [10,11]. This results in poor oxidation resistance and coating delamination along their cutting edges. When the bottom layer of Al₂O₃ is exposed, the wear resistance increases and the flank wear become stable after machining a length of 15 cm as shown in Fig 2. It exhibited abrasion and adhesion wear mechanism along with oxidation wear as shown in Fig. 3 (c). The adhesion of work material and coating delamination exposing the tungsten substrate shown by elemental mapping is depicted in Figs.7 (a) (b) and (c).

In TiOCN- Al₂O₃ -TiCN-[MT-TiCN]-TiN coating the top titanium oxy carbo-nitride is chemically very inert, and it retains its hardness at high temperature, that helps to resist the abrasion. Fig. 3 (d) depicts the predominant

wear mode is abrasion. It provides lesser oxidation resistance, but the enhancement in hardness level makes it as an effective coating layer in industrial applications. Fig. 8 (c) shows the traces of iron element along the cutting edges, but still it is not strong enough to favor any strong built-up edges that affect the efficiency of tool. From Figs. 8 (a) and 7 (b) it is evident that complex oxide formation along the edges helps in preventing deformation of coating. The TiN layer at bottom of this coating provides good adhesion that can act as an intermediate layer between tungsten carbide substrate and other layers in these coatings. This coated tool showed a better wear resistance next to [MT-TiCN]-Al₂O₃ coating.

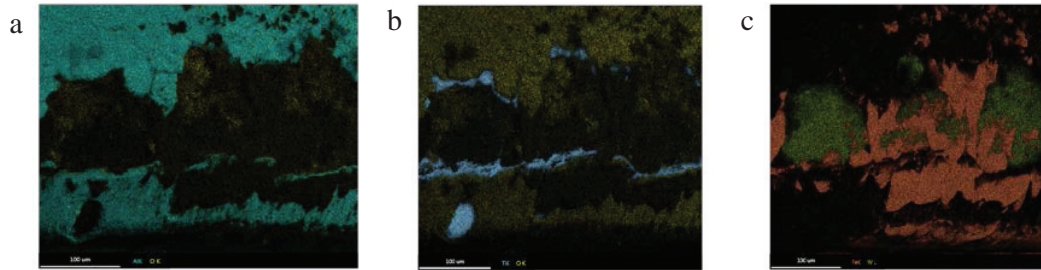


Fig. 7. EDS showing the elemental mapping for ROI (red box) the coating TiN-[MT-TiCN]-Al₂O₃ :
a)Al- ■, O- ■ (b) Ti- ■, O- ■ (c) Fe- ■, W- ■

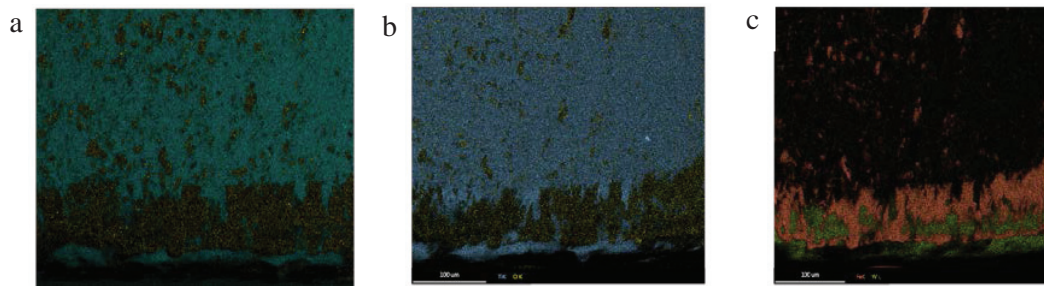


Fig. 8. EDS showing the elemental mapping for the ROI (red box) TiOCN(Top)-Al₂O₃-TiCN-[MT-TiCN]-TiN:
a)Al- ■, O- ■ (b) Ti- ■, O- ■ (c) Fe- ■, W- ■

3.2 Cutting Force

The cutting forces were measured along two axes, F_x & F_z (Axial feed force and Tangential force) respectively. The higher percentage of molybdenum as seen in Table 1 increases the strength of material at higher temperature. These elements make this material difficult-to-machine and it is primarily responsible for the higher cutting forces generated during machining as seen in Fig. 9. The TiN-[MT-TiCN]-Al₂O₃ coating exhibited high level of forces for shearing the material, among all the four different coatings. The relatively high coefficient of friction of top TiN layer and the higher tool wear caused increased forces. The measured forces were not uniform, which is due to the non-continuous progression of tool wear along the cutting edge. Hence it's been specifically mentioned in Fig. 10. The [MT-TiCN]-Al₂O₃ coating showed second highest forces among the four different tools. The coating exhibited lower levels of flank wear due to high hardness of TiCN during initial stages of machining. However, with increasing cutting temperatures reduction of hardness was observed which resulted in increased forces. Further, the second layer Al₂O₃ with high coefficient of friction also favoured increased forces. TiOCN-Al₂O₃-TiCN-[MT-TiCN]-TiN coating did by PVD provide lower magnitude of cutting force among all the four different coatings. The addition of oxygen in TiCN layer forms an interstitial layer of titanium oxy carbo-niride, where oxygen and carbon atoms replace the nitrogen atom in their lattice site. This layer provides higher hardness and very low friction of

TiOCN layer at the top, which resulted in increased resistance to wear and lower cutting forces. The AlTiN has high coefficient of friction than TiOCN layer, hence high forces were observed with machining AlTiN coating.

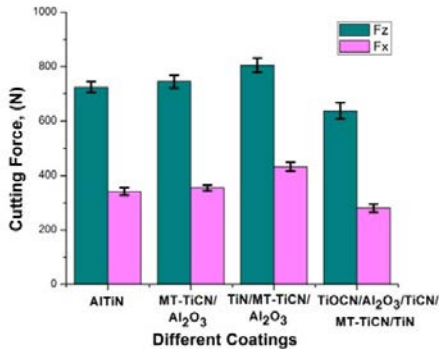


Fig. 9. Average Cutting Forces

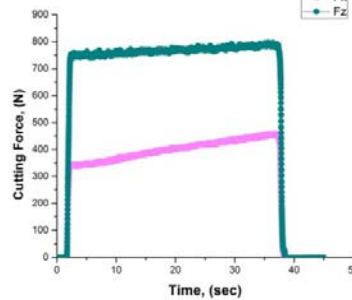


Fig. 10. Cutting force for TiN-[MT-TiCN]- Al₂O₃ coating

3.3 Cutting Temperature

The Temperature is measured at the tool chip interface, when the tool machined over a length of 15 cm along the work piece for each different coated tools as shown in Fig. 11. The high temperature generated during machining, affects the dimensional accuracy of work piece and it can also induce thermal stresses into the work piece. The Fig. 11 also shows that AlTiN coating generated higher temperature than other coatings and it could be due to the higher friction coefficient of their coating layer.

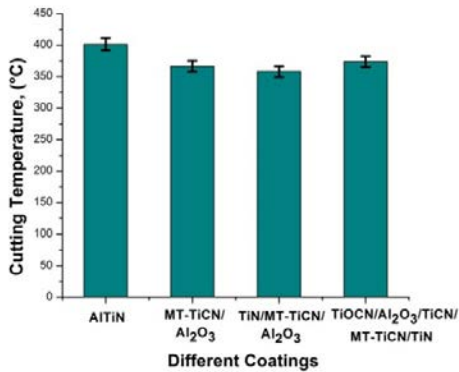


Fig. 11. Cutting Temperature

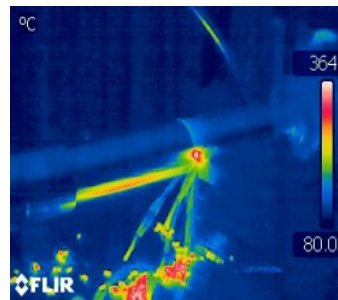


Fig. 12. Infra-Red (IR) image of Measured Temperature

It resists the incoming heat into the layer and transfers the heat back into the chip. In addition, the Al₂O₃ protective layer provides exceptional oxidation resistance makes them effective in high temperature applications. [MT-TiCN]- Al₂O₃ and TiOCN-Al₂O₃-TiCN-[MT-TiCN]-TiN exhibited smaller difference in their temperature level between them. Since both coatings have TiCN in their top layer, the similarity in their friction and hardness values resulted in similar temperature ranges. The TiN top layer of TiN-[MT-TiCN]- Al₂O₃ coating provides better thermal resistance than TiCN, this could have resulted less temperature. Fig. 12 shows the Infra-Red image of measured temperature at the tooltip. Overall temperature study indicates that there is a small difference in their measured temperature range other than AlTiN coating.

3.3 Surface Integrity:

3.3.1 Residual Stress

The surface integrity primarily involves surface topography and internal subsurface features such as micro-hardness, residual stress of a machined component. In this work, it has been analyzed by measuring the surface roughness and internal stress distribution after machining the SDSS. During machining, the residual stresses are generated at the surface due to the plastic deformation caused by the mechanical loads and high temperature effects. The residual stress measurement helps to predict the quality of a machined surface, as the harmful stresses (tensile) can affect the functional performance such as fatigue strength and stress corrosion cracking. It was measured along both longitudinal direction and transverse direction. Even though all the coatings were machined with same process parameter, the work material exhibited a high difference in their surface residual stress. The measured stresses were tensile in nature on all the work surfaces as shown in Fig. 13. This indicates that high temperature generated during machining is primarily responsible for introducing high tensile residual stresses on all the work surfaces. The high difference in coefficient of thermal expansion between ferrite and austenite causes non-uniform cooling, which subsequently increases the level of tensile stress distribution across their microstructure [7]. The machining done by AlTiN coating showed high tensile residual stresses on SDSS surface. It could be attributed to the very poor thermal conductivity of AlTiN layer. The Al_2O_3 formed prevents the heat dissipation into the tool substrate and reflects the heat energy back into cutting zone. This increases the amount of heat conducted into work surface and causes increased tensile stress. The surface machined with TiN-[MT-TiCN]- Al_2O_3 tool exhibited the lowest levels of tensile residual stresses among all the four different coating studied. The top two Ti based layers with relatively higher thermal conductivity and coating delamination could have resulted in more heat penetration in to the tool substrate. This leads to a lesser tensile stresses on the machined surface. The high cutting force generated by this coating also shows the dominance of plastic deformation by mechanical load over temperature effects that reduced the tensile stress.

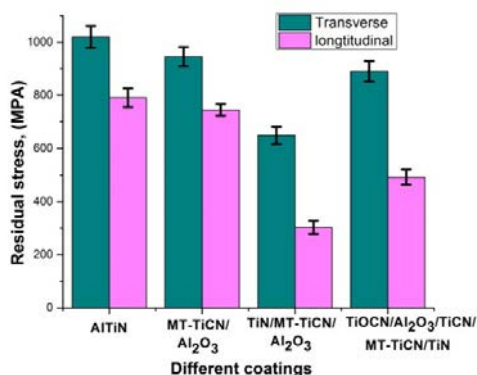


Fig. 13. Residual stress By X ray Diffraction technique

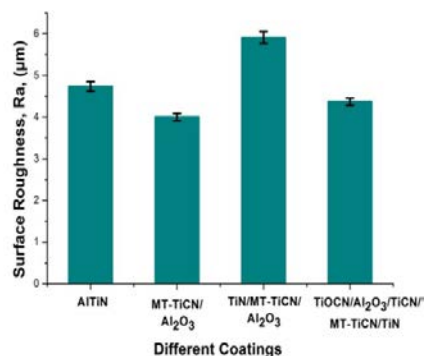


Fig. 14. Surface Roughness

The (MT-TiCN) / Al_2O_3) and TiOCN- Al_2O_3 -TiCN-[MT-TiCN]-TiN showed little difference in residual stress measured. This could be because of their similarity in top two layers either TiCN or TiOCN followed by Al_2O_3 with relatively similar cutting temperature observed during machining.

3.3.2 Surface Roughness

The Surface roughness of the work material after machining was measured by 3-D noncontact optical surface profiler. The roughness profiles of work piece after machining were taken at five spots and their average values are shown in Fig 14. The obtained images by white light interferometry technique for different coatings are shown in Fig 15. During machining, the work material got adhered to the cutting edge and formed built up edge that affected the surface finish in all the machined surfaces. The TiN-[MT-TiCN]- Al_2O_3 coating exhibited poor surface finish among the four coatings because of higher tool wear. Fig. 15 (c) shows surface texture is not uniform for the machining done using this coating. This could be due to the non-uniformity in cutting edges as TiN coating gets peeled off during machining because of their low hardness. The machined surface was also analyzed by the SEM to

study the defects and irregularities in the surface. Particles as a result of built-up edge were found between feed marks on all the work surfaces after machining. High surface irregularities and large sized wear debris particles were found on the machined surface machined by The TiN-[MT-TiCN]-Al₂O₃ coating seen in Fig. 16 (c). The machined surface by [MT-TiCN]- Al₂O₃ coating showed better surface finish among all other coatings, because of low friction coefficient of TiCN layer and their higher resistance to flank wear. Fig 15 (b) shows the observed texture is uniform

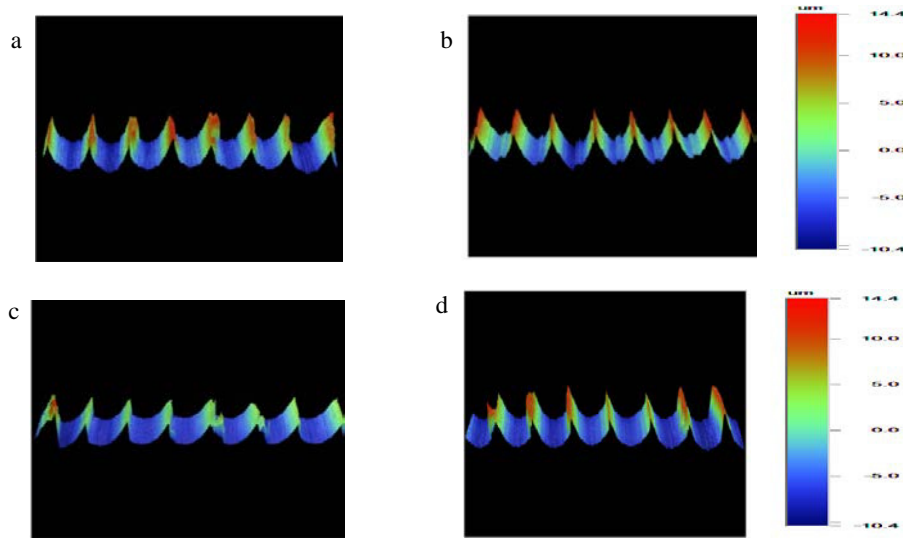


Fig. 15. 3D image of surface obtained for different coatings respectively

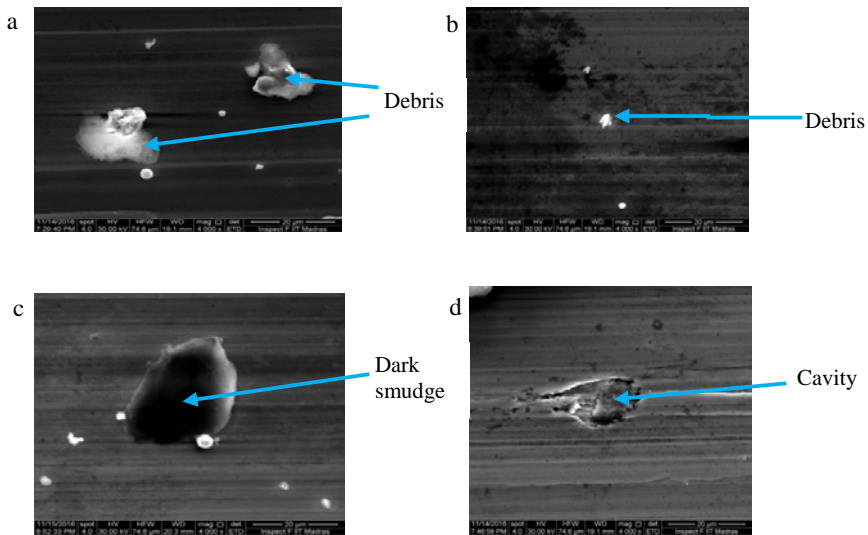


Fig. 16. SEM image of surface obtained for different coatings respectively

and parallel in comparison with other surfaces. The work surface also had relatively lesser residues and they were smaller in size as shown in 16 (b).It is followed by TiOCN- Al₂O₃ -TiCN-[MT-TiCN]-TiN coating. The scattered debris were found lesser with a cavity in few areas as shown in 16 (d).The coated tool AlTiN exhibited lesser wear

but higher built-up edge formation resulted in poor surface with lots of debris on the work surface indicated in Fig 16 (a).

4. Conclusion

In this study, the performance of different coated tools were investigated while machining superduplex stainless steel (SDSS). The performance was analyzed in terms of tool wear, cutting force, cutting temperature and surface integrity of the work surface.

- The tool wear study showed that [MT-TiCN]-Al₂O₃ coated tool provided good wear resistance among all coatings. The higher hardness of MT-TiCN and oxidation stability of Al₂O₃ at the interface provided increased wear resistance among other coatings. It is followed by TiOCN- Al₂O₃ -TiCN-[MT-TiCN]-TiN and AlTiN.
- TiN-[MT-TiCN]- Al₂O₃ exhibited higher level of forces among different coatings. The measured forces also showed fluctuations, which is due to the non-continuous progression of tool wear. TiOCN- Al₂O₃ -TiCN-[MT-TiCN]-TiN coating provides lower of magnitude of forces as the higher hardness of TiOCN and their lower friction coefficient helps in easy shearing of work material.
- AlTiN coating generated higher temperature because of high friction and low thermal conductivity. Only small differences in temperature were observed in other coatings.
- The residual stress on the machined surface showed that the stresses were tensile for all the coatings studied, which can lead to failure. The machined surface by TiN-[MT-TiCN]-Al₂O₃ coating showed less tensile residual stress among the other surfaces due to the relatively dominance of plastic deformation by mechanical loads over the high temperature effects.
- The surface Roughness profile showed the [MT-TiCN]-Al₂O₃ coating exhibited lower roughness (Ra) values because of their higher resistance to abrasion along the cutting edges and surface had less residues in comparison with other surfaces.
- From the above study it is suggested that [MT-TiCN]-Al₂O₃ coating provided relatively better performance in-terms of tool wear, cutting force, cutting temperature and surface integrity than other coatings followed by TiOCN- Al₂O₃ -TiCN-[MT-TiCN]-TiN and coatings.

References

- [1] Koyee Rastee, Uwe Heisela, Rocco Eisselera and Siegfried Schmauder, Modeling and optimization of turning duplex stainless steels. *Journal of Manufacturing Processes*, 16.4, (2014) 451-467.
- [2] Nian Zhou. Surface integrity of 2304 duplex stainless steel after different grinding operations. *Journal of Materials Processing Technology*, 229, (2016) 294-304.
- [3] Nomani J, Pramanik A, Hilditch T and Littlefair, Machinability study of first generation duplex (2205), second generation duplex (2507) and austenite stainless steel during drilling process. *Wear*, 304.1, (2013) 20-28.
- [4] S. PalDey, S.C. Deevi, Single layer and multilayer wear resistant coatings of (Ti,Al)N: a review. *Materials Science and Engineering*, A342, (2003) 58/79.
- [5] H.G prenge, Heinrich, Roder, CVD coatings based on medium temperature CVD Al₂O₃. *Surface and coating technology*, 68/69, (1994) 217-220.
- [6] Anongsack Paseuth, Haruyo Fukui and Kazuo Yamagata. Improvement of mechanical properties and cutting performance of modified MT-TiCxN1-x coating by moderate temperature chemical vapor deposition. *Surface and Coatings Technology*, 291, (2016) 54-61.
- [7] Johansson J, Odén M, Zeng XH, Evolution of the residual stress state in a duplex stainless steel during loading. *Acta mater*, 47, (1999) 2669-84.
- [8] Krolczyk G. M., Nieslony P and Legutko S, Determination of tool life and research wear during duplex stainless steel turning. *Archives of Civil and Mechanical Engineering*, 15.2, (2015) 347-354.
- [9] Królczyk, Grzegorz, Stanisław Legutko and Pero Raos, Cutting wedge wear examination during turning of duplex stainless steel. *Tehnički Vjesnik-Technical Gazette*, 20.3, (2013) 413-418.
- [10] Jihua Peng, Dongyi Su and Chengxi Wang, Combined Effect of Aluminum Content and Layer Structure on the Oxidation Performance of Ti1LxAlxN Based Coatings. *J. Mater. Sci. Technol*, 30(8), (2014) 803-807.

- [11] Li Chen, Yong Du, Xiang Xiong, Improved properties of Ti-Al-N coating by multilayer structure. *Int. Journal of Refractory Metals and Hard Materials*, 29, (2011) 681–685.
- [12] J.H. Hsieh, A.L.K. Tan and X.T. Zeng, Oxidation and wear behaviors of Ti-based thin films. *Surface & Coatings Technology*, 201, (2006) 4094–4098.
- [13] Ibrahim Ciftci, Machining of austenitic stainless steels using CVD multi-layer coated cemented carbide tools. *Tribology International*, 39, (2006) 565–569.
- [14] Bejjani, M and Collin. Three dimensional topographic studies on worn surfaces of coated cemented carbide tools with different workpiece materials. *CIRP Journal of Manufacturing Science and Technology*, (2016).
- [15] Kyung-Hee Parka and Patrick Y. Kwon., Flank wear of multi-layer coated tool. *Wear* 270, (2011) 771–780.
- [16] Youqiang Xing, Jianxin Deng, Shipeng Li, Hongzhi Yue, Rong Meng and Peng Gao. Cutting performance and wear characteristics of Al_2O_3/TiC ceramic cutting tools with WS 2/Zr soft-coatings and nano-textures in dry cutting. *Wear*, 318.1, (2014) 12-26.
- [17] W. Grzesik and P. Nieslony. Thermal Characterization of the Chip-Tool Interface When Using Coated Turning Inserts. *Journal of Manufacturing Processes*, Vol. 2/No, (2000) 2-2000.
- [18] J.L. Endrino, G.S. Fox-Rabinovich and C. Gey. Hard AlTiN, AlCrN PVD coatings for machining of austenitic stainless steel. *Surface & Coatings Technology*, 200, (2006) 6840–6845.